

Photoluminescence of $[\text{Eu}(\text{bpy})_2]^{3+}$ dispersed in MCM-41 and HMS

Ge Shuxun¹ He Nongyue^{1,2}

(¹Key Laboratory of Molecular and Bio-Molecular Electronics of Ministry of Education, Southeast University, Nanjing 210096, China)

(²School of Packing and Printing, Zhuzhou Institute of Technology, Zhuzhou 412008, China)

Abstract: $[\text{Eu}(\text{bpy})_2]^{3+}$ (bpy: 2, 2'-bipyridine) was encapsulated in hexagonal mesoporous materials MCM-41 and HMS. XRD spectra, ICP analysis, IR spectra, N_2 adsorption measurements and the photoluminescence spectra were used to characterize the corresponding impregnated samples. After the impregnation of $[\text{Eu}(\text{bpy})_2]^{3+}$, the BET surface, pore diameters and pore volume of the impregnated samples were decreased. All the impregnated samples exhibited the typical photoluminescence of Eu^{3+} when excited with a xenon lamp. Compared with the impregnated HMS, the impregnated MCM-41 samples show higher photoluminescence efficiency for the impregnation of $[\text{Eu}(\text{bpy})_2]^{3+}$. It suggests that MCM-41 is a more efficient host for the photoluminescence of europium complexes than HMS.

Key words: nanostructures; optical materials; optical properties; surface properties

The typical structural properties of zeolites, i. e., well-defined channels and pore diameters, are ideal for hosting for guest ions or molecules with specific chemical and optical properties, providing a challenging approach to novel chemical and optical applications^[1,2]. However, the microporous structures of zeolites restrict themselves to assembled supermolecules. M41S materials^[3] have promising potential for utilisation in assembling optoelectronics materials due to their high surface area (about 1 000 m^2/g), large pore volume and mesoporous pore diameters (2 to 50 nm). Rare earth complexes, especially Eu^{3+} complexes, have been studied for practical applications. These complexes must be incorporated into a stable rigid matrix in order to make these materials applicable for technological use. There are a few reports on the photoluminescence (PL) properties of europium complexes immobilized in pure or organically modified hexagonal MCM-41^[4–10] and cubic MCM-48^[11]. HMS synthesized by the assembly pathway of hydro-bonding interactions between neutral primary amine and inorganic precursors is distinguishable from MCM-41 in part by its framework wall, domain size and textural mesoporosity^[12]. The differences in the structure of mesoporous materials can result in different PL efficiency of the corresponding impregnated samples. In this paper, we focus on the PL properties of $[\text{Eu}(\text{bpy})_2]^{3+}$ dispersed in MCM-41 and HMS,

and on the PL efficiency of the hosts for the impregnation of $[\text{Eu}(\text{bpy})_2]^{3+}$.

1 Experimental

MCM-41 and HMS were synthesized and calcined as given in Refs. [13, 14]. A controlled amount of $[\text{Eu}(\text{bpy})_2]^{3+}$ was dissolved in 10 cm^{-3} of N, N-dimethylformamide (DMF) and calcined MCM-41 was suspended in this solution, then it was stirred vigorously at room temperature for 24 h. Solutions with different concentrations of $[\text{Eu}(\text{bpy})_2]^{3+}$ were employed for the impregnation. The initial $[\text{Eu}(\text{bpy})_2]^{3+}/\text{MCM-41}$ mass ratios were 0.05, 0.10, and 0.20. The obtained samples were designated as 5% Eu-MCM-41, 10% Eu-MCM-41 and 20% Eu-MCM-41, respectively. After the impregnation, the solid product was recovered by filtration, washed with DMF, dried at 100 $^{\circ}\text{C}$ for 10 h and finally kept in a vacuum desiccator. Furthermore, 5% Eu-HMS, 10% Eu-HMS and 20% Eu-HMS were prepared by the same method.

Powder X-ray diffraction (XRD) patterns of the samples were recorded on a Rigaku D/max-rB diffractometer using $\text{Cu K}\alpha$ radiation and scanning in the 2θ range of 1° to 10° . The framework vibration infrared (IR) spectra were recorded on a Nicolet Magna 750FT-IR spectrometer with a resolution 2 cm^{-1} . The PL spectra were recorded on a Perkin Elmer LS50B spectrofluorometer in the wavelength range of 320 to 800 nm using an excitation wavelength of 300 nm with a xenon lamp. The spectra were measured with a 350 nm filter to block out the excitation signal. Both the excitation and emission slit widths were kept as 5.0 nm. N_2 ad-

Received 2005-03-08.

Foundation items: The Open Project of National Laboratory of Solid State Microstructures, Trans-Century Training Programme Foundation for the Talents by the State Education Commission.

Biographies: Ge Shuxun (1976—), male, graduate; He Nongyue (corresponding author), male, doctor, professor, nyhe1958@163.com.

sorption/desorption isotherms were determined by using a Micromeritics ASAP2010 Chemisorption Analyzer. Surface areas, total pore volumes and pore size distributions were extracted from these isotherms using the BET and BJH methods, respectively. The contents of Eu^{3+} in the assemblies were analyzed on a Leeman PS-1 ICP instrument.

2 Results and Discussion

Fig. 1 shows the powder XRD patterns of MCM-41 host, 5% Eu-MCM-41, 10% Eu-MCM-41 and 20% Eu-MCM-41. The patterns of MCM-41 host features distinct 100, 110, 200 and 210 peaks in the 2θ range of 1° to 10° , in agreement with well-defined structural regularity of MCM-41^[13]. The influence of $[\text{Eu}(\text{bpy})_2]^{3+}$ content on the structural regularity of MCM-41 is clearly illustrated. The XRD patterns of the impregnated MCM-41 samples are less regular compared to that of the host. With the increase of $[\text{Eu}(\text{bpy})_2]^{3+}$, the structural order of the impregnated MCM-41 samples decreases. This reveals that the impregnation of $[\text{Eu}(\text{bpy})_2]^{3+}$ can induce the decrease in the structure order of MCM-41.

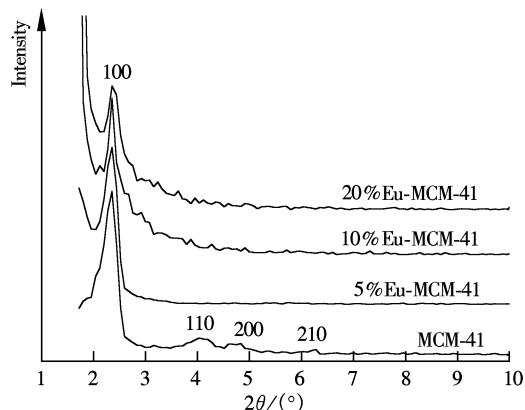


Fig. 1 Powder XRD patterns of MCM-41 and impregnated samples

Tab. 1 summarizes the textural properties of mesoporous hosts before and after the impregnation of $[\text{Eu}(\text{bpy})_2]^{3+}$. The MCM-41 shows somewhat larger BET surface and pore volume than HMS. However, the pore diameter of MCM-41 is smaller than that of HMS. The pore diameter for MCM-41 and HMS is 3.13 and 4.59 nm, respectively. The surface area, pore volume and pore diameter of impregnated MCM-41 samples decrease due to the impregnation of $[\text{Eu}(\text{bpy})_2]^{3+}$. Moreover, the decrease in structural parameters was observed in the order of content of $[\text{Eu}(\text{bpy})_2]^{3+}$. The relevant structural parameters for the impregnated HMS products are provided (as shown in Tab. 1). Also, a substantial decrease in the pore parameters was realized after the impregnation of

$[\text{Eu}(\text{bpy})_2]^{3+}$. It was suggested that the impregnation of $[\text{Eu}(\text{bpy})_2]^{3+}$ could induce the decrease of pore parameters, which could be expected due to the fact that $[\text{Eu}(\text{bpy})_2]^{3+}$ remained in the host after the impregnation and washing.

Tab. 1 Textural properties of mesoporous hosts before and after the impregnation of $[\text{Eu}(\text{bpy})_2]^{3+}$

Sample	BET surface/ ($\text{m}^2 \cdot \text{g}^{-1}$)	Pore volume/ ($\text{cm}^3 \cdot \text{g}^{-1}$)	Pore diameter/nm
MCM-41	961.9	0.75	3.13
5% Eu-MCM-41	844.2	0.65	3.08
10% Eu-MCM-41	793.4	0.61	3.06
20% Eu-MCM-41	472.1	0.60	3.05
HMS	644.7	0.74	4.59
5% Eu-HMS	604.6	0.69	4.56
10% Eu-HMS	595.5	0.66	4.43
20% Eu-HMS	450.4	0.50	4.44

Infrared spectra of $[\text{Eu}(\text{bpy})_2]^{3+}$ and the impregnated samples are shown in Fig. 2. All the impregnated MCM-41 samples show the same silica framework infrared absorption bands. The strongest absorption bands relative to the silica host structure appear in the 1000 to 1250 cm^{-1} range due to asymmetric Si—O stretching vibration modes, whereas the peak at 800 cm^{-1} can be attributed to the symmetric Si—O stretching vibration^[8, 11]. The Si—O—Si bending vibration can be observed at 459 cm^{-1} , and the bands at 959 cm^{-1} can be assigned to stretching vibrations of Si—OH surface groups^[15]. In addition, the presence of water molecules is clearly evidenced by two strong absorption bands peaking at 1653 and 3445 cm^{-1} . The most interesting features concerning the impregnated samples are observed in the 1440 cm^{-1} wavenumber band, which was connected to the organic part interacting with the host structure^[11]. The intensity of the band increased with the increase of $[\text{Eu}(\text{bpy})_2]^{3+}$ in the MCM-41 host, see Fig. 2.

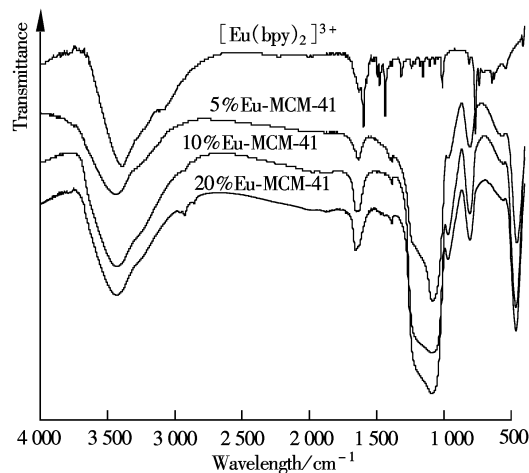


Fig. 2 IR spectra of europium complexes and impregnated samples

The PL spectra of impregnated MCM-41 samples are exhibited in Fig. 3. All the impregnated samples exhibit two main PL peaks at the red light region that originated from $^5\text{D}_0 \rightarrow ^7\text{F}_1$ ($\lambda = 589 \text{ nm}$) and $^5\text{D}_0 \rightarrow ^7\text{F}_2$ ($\lambda = 612 \text{ nm}$) of Eu^{3+} , respectively. It seems to indicate that the electron transition energy of Eu^{3+} was not affected by silica^[5]. The contents of Eu^{3+} in 5% Eu-MCM-41, 10% Eu-MCM-41, and 20% Eu-MCM-41 measured by ICP are 0.21%, 0.29%, and 1.44%, respectively. Based on the PL efficiency equation, i. e., PL efficiency = (the PL intensity of PL peak at 612 nm)/(the content of Eu^{3+}), the PL efficiency of impregnated MCM-41 samples are higher than the pure $[\text{Eu}(\text{bpy})_2]^{3+}$ complexes (as shown in Tab. 2). This result suggests that mesoporous materials may prevent the PL quenching of rare earth ions^[5].

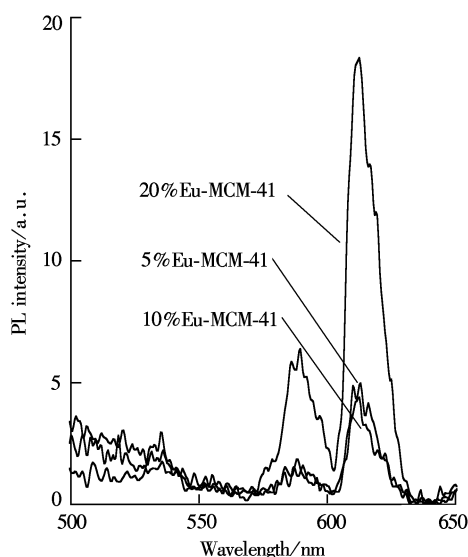


Fig. 3 PL spectra of impregnated samples

Tab. 2 PL properties of impregnated MCM-41 and HMS

Sample	Content of europium/%	PL intensity/ (a. u.)	PL efficiency
$[\text{Eu}(\text{bpy})_2]^{3+}$	41.58	136.00	3.27
5% Eu-MCM-41	0.21	4.86	23.14
10% Eu-MCM-41	0.29	4.44	15.30
20% Eu-MCM-41	1.44	18.30	12.71
5% Eu-HMS	0.20	1.17	5.85
10% Eu-HMS	0.99	4.74	4.79
20% Eu-HMS	1.80	7.87	4.36

The PL efficiency of the impregnated HMS samples is higher than that of the pure $[\text{Eu}(\text{bpy})_2]^{3+}$ complexes. However, the PL efficiency of the impregnated HMS is weaker than that of the impregnated MCM-41. This difference in the PL efficiency may result from the differences in the synthesis conditions. The assembly mechanism can affect the condensation of silanol groups^[16]. Furthermore, the mechanism of

the synthesis of MCM-41 and HMS is (S^+I^-) and (S^0I^0) , respectively. In the (S^+I^-) mechanism, a high condensation of silanol groups to highly polymerized $\text{Si}-\text{O}-\text{Si}$ bonds is catalyzed by the counterions where as in the (S^0I^0) mechanism no such condensation promoter is available in the reaction medium. Therefore, the (S^+I^-) assembled silica mesostructures which consist of better-polymerized walls may result in lower silanol content. In addition, silanol groups in the mesoporous materials can quench photoluminescence^[4]. This suggests that the low content of silanol groups may be one of the factors affecting the PL efficiency. It is further believed that MCM-41 is a more efficient host for the encapsulation of the rare earth complexes than HMS.

3 Conclusion

Hexagonal mesoporous materials MCM-41 and HMS impregnated with $[\text{Eu}(\text{bpy})_2]^{3+}$ complex were prepared and characterized. The impregnation of $[\text{Eu}(\text{bpy})_2]^{3+}$ induced the decrease of the structure order and the pore parameters of the hosts. All the encapsulated samples exhibited the typical photoluminescence of Eu^{3+} when excited with a xenon lamp. Compared with the impregnated HMS samples, the corresponding impregnated MCM-41 showed higher PL efficiency. This result shows that MCM-41 is a more efficient host lattice for the impregnation of $[\text{Eu}(\text{bpy})_2]^{3+}$ than HMS. Our results suggest that MCM-41 is suitable for future optoelectronic applications as a host.

References

- [1] Maas H, Currao A, Calzaferri G. Encapsulated lanthanides as luminescent materials [J]. *Angewandte Chemie-International Edition*, 2002, **41**(14): 2495 – 2497.
- [2] Brühwiler D, Calzaferri G. Molecular sieves as host materials for supramolecular organization [J]. *Microporous Mesoporous Materials*, 2004, **72**(1–3): 1 – 23.
- [3] Kresge C T, Leonowicz M E, Roth W J, et al. Ordered mesoporous molecular sieves synthesized by a liquid-crystal template mechanism [J]. *Nature*, 1992, **359**(6397): 710 – 712.
- [4] Li H R, Lin J, Fu L S, et al. Phenanthroline-functionalized MCM-41 doped with europium ions [J]. *Microporous Mesoporous Materials*, 2002, **55**(1): 103 – 107.
- [5] Bian L J, Xi H A, Qian X F, et al. Synthesis and luminescence property of rare earth complex nanoparticles dispersed within pores of modified mesoporous silica [J]. *Materials Research Bulletin*, 2002, **37**(14): 2293 – 2301.
- [6] Xu Q H, Li L S, Li B, et al. Encapsulation and luminescent

- property of tetrakis (1-(2-thenoyl)-3, 3, 3-trifluoroacetate) europium N-hexadecyl pyridinium in modified Si-MCM-41 [J]. *Microporous Mesoporous Materials*, 2000, **38**(2, 3): 351 – 358.
- [7] Yin Wei, Zhang Maisheng, Kang Beisheng. Encapsulation of the functional supramolecular NSM of rare earth and its comparison of fluorescence [J]. *Chinese Journal of Inorganic Chemistry*, 2001, **17**(1): 60 – 64. (in Chinese)
- [8] Zhang M S, Yin W, Su Q, et al. Encapsulation and luminescence of the nanostructured supramolecular material [Eu(Phen)₄](NO₃)₃/(CH₃)₃Si-MCM-41 [J]. *Materials Letters*, 2002, **57**(4): 940 – 945.
- [9] Fu L S, Xu Q H, Zhang H J, et al. Preparation and luminescence properties of the mesoporous MCM-41s intercalated with rare earth complex [J]. *Materials Science and Engineering B-solid state materials for advanced technology*, 2002, **88**(1): 68 – 72.
- [10] Gleizes A N, Fernandes A, Dexpert-Ghys J. Grafting 4f and 3d metal complexes into mesoporous MCM-41 silica by wet impregnation and by chemical vapour infiltration [J]. *Journal of Alloys and Compounds*, 2004, **374**(1, 2): 303 – 306.
- [11] Meng Q G, Boutinaud P, Franville A C, et al. Preparation and characterization of luminescent cubic MCM-48 impregnated with an Eu³⁺ beta-diketonate complex [J]. *Microporous Mesoporous Materials*, 2003, **65**(2, 3): 127 – 136.
- [12] Yin D H, Li W H, Yang W S, et al. Mesoporous HMS molecular sieves supported cobalt catalysts for Fischer-Tropsch synthesis [J]. *Microporous Mesoporous Materials*, 2001, **47**(1): 15 – 24.
- [13] Yang C, Ge S X, He N Y. A further investigation on effect of basic media on the synthesis of MCM-41 [J]. *Studies in Surface Science and Catalysis*, 2002, **146**: 129 – 132.
- [14] Yang C, Jia X P, Cao Y D, et al. Functionalization of hexagonal mesoporous silica and their base-catalytic performance [J]. *Studies in Surface Science and Catalysis*, 2002, **146**: 485 – 488.
- [15] He N Y, Yuan C W, Lu Z H, et al. The very strong photoluminescent (PL) effect of mesoporous molecular sieve materials [J]. *Supramolecular Science*, 1998, **5**(5, 6): 523 – 526.
- [16] Cassiers K, van der Voort P, Linssen T, et al. A counterion-catalyzed ((S⁰H⁺)(X⁻I⁺) pathway toward heat-and steam-stable mesostructured silica assembled from amines in acidic conditions [J]. *Journal of Physical Chemistry B*, 2003, **107**(16): 3690 – 3696.

MCM-41 和 HMS 孔内组装 [Eu(bpy)₂]³⁺ 及其光致发光性质

葛树勋¹ 何农跃^{1,2}

(¹ 东南大学分子与生物分子电子学教育部重点实验室, 南京 210096)

(² 株洲工学院包装与印刷学院, 株洲 412008)

摘要: 采用浸渍的方法在 MCM-41 和 HMS 介孔材料孔内组装 [Eu(bpy)₂]³⁺ (bpy: 2, 2'-联吡啶)。所得介孔复合材料经 XRD、ICP 等离子发射光谱、IR、N₂ 吸附实验及光致发光谱进行了表征。实验结果表明: 与介孔材料母体相比, 组装稀土配合物后的介孔复合材料的 BET 比表面积、孔径和孔容均有所下降; 组装稀土配合物的介孔复合材料在氩光源激发下, 均发射出特征的 Eu³⁺ 光致发光谱; 与组装稀土配合物的 HMS 介孔复合材料相比, 组装后的 MCM-41 介孔复合材料具有较高的光致发光效率。MCM-41 介孔材料是一种比 HMS 合适的载体, 有助于增强介孔材料孔内组装稀土配合物的光致发光效率。

关键词: 纳米结构; 光学材料; 光学性质; 表面性质

中图分类号: O433. 3